



Published in final edited form as:

Nature. ; 480(7378): 530–533. doi:10.1038/nature10639.

## Adherens junction protein nectin-4 (PVRL4) is the epithelial receptor for measles virus

Michael D. Mühlebach<sup>1</sup>, Mathieu Mateo<sup>2</sup>, Patrick L. Sinn<sup>3</sup>, Steffen Prüfer<sup>1</sup>, Katharina M. Uhlig<sup>1</sup>, Vincent H. J. Leonard<sup>2</sup>, Chanakha K. Navaratnarajah<sup>2</sup>, Marie Frenzke<sup>2</sup>, Xiao X. Wong<sup>4</sup>, Bevan Sawatsky<sup>4</sup>, Shyam Ramachandran<sup>3</sup>, Paul B. McCray Jr.<sup>3</sup>, Klaus Cichutek<sup>1</sup>, Veronika von Messling<sup>4,5</sup>, Marc Lopez<sup>6</sup>, and Roberto Cattaneo<sup>2</sup>

<sup>1</sup> Division of Medical Biotechnology, Paul-Ehrlich-Institut, 63225 Langen, Germany

<sup>2</sup> Department of Molecular Medicine, Mayo Clinic, Rochester, Minnesota 55902, USA

<sup>3</sup> University of Iowa Carver College of Medicine, Iowa City, Iowa 52242, USA

<sup>4</sup> INRS and Institut Armand Frappier, University of Quebec, Laval, Quebec, Canada

<sup>5</sup> Duke University and National University of Singapore, Singapore

<sup>6</sup> INSERM, UMR891/CRCM and University of Aix-Marseille, 13009 Marseille, France

### Abstract

Measles (MV) is an aerosol-transmitted virus that affects more than 10 million children each year and accounts for approximately 120,000 deaths<sup>1,2</sup>. While it was long believed to replicate in the respiratory epithelium before disseminating, it was recently shown to initially infect macrophages and dendritic cells of the airways using the signaling lymphocytic activation molecule (SLAM, CD150) as receptor<sup>3-6</sup>. These cells then cross the respiratory epithelium and ferry the infection to lymphatic organs where MV replicates vigorously<sup>7</sup>. How and where the virus crosses back into the airways has remained unknown. Based on functional analyses of surface proteins preferentially expressed on virus-permissive epithelial cell lines, we identified nectin-4<sup>8</sup> (poliovirus-receptor-like-4) as a candidate host exit receptor. This adherens junction protein of the immunoglobulin superfamily interacts with the viral attachment protein with high affinity through its membrane-distal domain. Nectin-4 sustains MV entry and non-cytopathic lateral spread in well-differentiated primary human airway epithelial sheets infected basolaterally. It is down-regulated in infected epithelial cells, including those of macaque tracheas. While other viruses use receptors to enter hosts or transit through their epithelial barriers, we suggest that MV targets nectin-4 to emerge in the airways. Nectin-4 is a cellular marker of several types of cancer<sup>9-11</sup>, which has implications for ongoing MV-based clinical trials of oncolysis<sup>12</sup>.

---

Users may view, print, copy, download and text and data-mine the content in such documents, for the purposes of academic research, subject always to the full Conditions of use: [http://www.nature.com/authors/editorial\\_policies/license.html#terms](http://www.nature.com/authors/editorial_policies/license.html#terms)

#### Author contribution statement

VHJL and MDM conceived the project with RC, who coordinated research. VHJL, SP, KMU and MDM performed and evaluated screens, and validated nectin-4 as candidate receptor. ML contributed purified proteins, antibodies and cell lines, and advised about their use. MM and CKN characterized nectin-4 function biochemically and in cells. PLS, SR and PBMC planned and executed experiments with well-differentiated human epithelial sheets. MF, XXW, BS and VvM planned and executed monkey infection experiments and their analyses. RC, MM and MDM wrote the paper. VvM, KC, PBMC and ML corrected it.

Analysis of the spread of a wild type MV expressing the green fluorescent protein (GFP) in human airway well-differentiated epithelial sheets revealed that MV infects only columnar cells connected by the apical adhesion complex<sup>13</sup>. Thus we thought that MV might target an intercellular junctional protein to enter the airway epithelium. To narrow the search for this receptor, we initially compared genome-wide transcription in permissive (H358 and H441) and non-permissive (H23 and H522) airway epithelium cell lines<sup>13</sup>. For these cells high quality genome-wide microarray analyses are available (GEO microarray data GSE8332)<sup>14</sup>. We identified 175 transmembrane proteins preferentially expressed in permissive cells. Among these, we expressed cDNAs of 22 that either had top preferential expression ratios, or interesting biological characteristics. None of these proteins, including four claudins from the tight junction, and E-cadherin and nectin-3 from the adherens junction (**Supplementary Table 1**, footnote), conferred susceptibility to MV infection.

Next we performed a genome-wide expression analysis based on mRNA extracted from all seven epithelial cell lines from human airways or bladder previously characterized as permissive (3 lines) or not (4 lines)<sup>13</sup>. This time, we observed significant enrichment of 222 mRNAs for surface-associated proteins (GEO microarray data GSE32155). We selected 16 genes with high expression ratios in both screens, interesting biological characteristics, or both. In addition, we selected the genes with the top 12 expression ratios not already represented in the first analysis (for details see **Supplementary Table 1**). Non-permissive Chinese hamster ovary cells were transfected with expression plasmids and subsequently infected with GFP-expressing MV.

In one instance, we observed GFP expression followed by syncytia formation (**Figure 1a**, central panel). The plasmid transfected in these cells coded for adherens junction protein PVRL4/nectin-4. The corresponding mRNA had the 9<sup>th</sup> highest preferential expression ratio in the second screen (**Supplementary Table 1**, #9). Nectin-4 is a single pass type I transmembrane protein of the immunoglobulin superfamily<sup>8,15</sup>. Its long (3.7 kb) mRNA was initially detected only in human trachea among somatic tissues<sup>8</sup>, but a recent study documented expression in skin, lung, prostate, and stomach<sup>16</sup>.

We assessed the levels of nectin-4 protein expression in the seven epithelial cell lines used for gene expression profiling. FACS analyses with specific antibodies confirmed high levels of expression in the three cell lines permissive for MV infection (**Figure 1b**, top row). Three of the non-permissive cell lines did not express nectin-4, while the fourth showed variable expression levels (**Figure 1b**, bottom row). We also purchased four nectin-4 specific siRNAs, and assessed whether transfection of H358 cells with these affects MV entry. Indeed, three siRNAs strongly reduced infection, and in particular siRNA 4\_1 almost completely abolished it (**Figure 1c**, right panel). We then documented that nectin-4 is functionally equivalent to the proposed epithelial receptor EpR<sup>13</sup> through cell fusion assays (**Supplementary Fig. 1**). We also showed that neither the other three human nectins nor the related poliovirus receptor PVR/CD155<sup>17</sup> have MV receptor function (**Supplementary Fig. 2**). Remarkably, alpha-herpesviruses use ubiquitous nectin-1 as receptor, and the same is true for nectin-2<sup>18</sup>. While this paper was in review, another group documented in cancer cells that nectin-4 is an epithelial cell receptor for MV<sup>19</sup>.

All four nectins share the same overall structure defined by three extracellular immunoglobulin-like domains (V and two C2-type domains, VCC), a single transmembrane helix, and an intracellular domain. To map the domain interacting with MV H, we took advantage of two recombinant soluble forms of nectin-4: VCC-Fc and the shorter V-Fc<sup>15</sup>, which were used to block MV infection. As shown in **Figure 2a**, both forms were similarly effective: 1 µg/ml solutions sufficed for about 50% reduction of syncytia formation.

An independent mapping approach relied on two nectin-4 specific antibodies, N4.40 and N4.61. While N4.40 recognizes one of the two C domains, N4.61 recognizes the V domain<sup>15</sup>. Again, different dilutions of either antibody were added before virus inoculation. **Figure 2b** shows that while a 0.5 µg/ml N4.61 solution inhibited entry almost completely, 100 times more concentrated N4.40 did not inhibit virus entry. Thus the soluble nectin-4 V domain and anti-V antibodies block infection.

To further characterize the interactions of soluble H and purified virus particles with nectin-4 and SLAM, we separated the same amount of soluble forms of both receptors by non-reducing polyacrylamide gel electrophoresis, and transferred them to membranes. **Figure 2c** documents that binding of H to partially denatured nectin-4 (2<sup>nd</sup> and 3<sup>rd</sup> lanes) is at least as strong as binding to partially denatured SLAM (1<sup>st</sup> lane). **Figure 2d** documents stronger binding of virus (left panel) and of soluble H protein (top right panel) to VCC-Fc than to V-Fc nectin-4 (left panel).

We then sought to determine the kinetic parameters of binding native nectin-4 (VCC-Fc) to native H. The soluble complete extracellular domain of SLAM was used as control (**Figure 2e**). The measured dissociation constant ( $K_d$ ) of SLAM was 93.5 nM, which compares well with 80 nM measured previously<sup>20</sup>. The  $K_d$  of H and nectin-4 was 20 nM: while the  $k_{off}$  of both reactions was similar, the  $k_{on}$  of nectin-4 and H was almost 5 times faster than that of SLAM and H (**Figure 2f**). Since the  $K_d$  of the CD46 and vaccine H interaction is about 79 nM<sup>20</sup>, nectin-4 is the cellular protein bound by H with strongest affinity. However, when CHO cells stably expressing either SLAM or nectin-4 were infected, we documented about 5 times more efficient MV infection in the SLAM-expressing CHO cells (**Supplementary Fig. 3**). Thus parameters other than the  $K_d$ , like accessibility of the receptor-binding region, influence virus spread in this system.

To assess the relevance of nectin-4 expression for MV infection in humans, we relied on primary human airway epithelial cells cultured at an air-liquid interface<sup>21</sup>. These cellular sheets closely resemble the human airway: cells develop apical adhesion complexes with tight and adherens junctions, and a well-differentiated morphology consisting of a pseudostratified, ciliated columnar epithelium with goblet and basal cells. In these epithelia, we confirmed nectin-4 mRNA expression (**Figure 3a**) at levels slightly higher than those of the Calu3 cell line, which supports efficient MV infection<sup>22</sup>. We next transfected the epithelia with specific siRNAs, achieving 90% decrease in nectin-4 mRNA (**Figure 3b**). We then infected the cultures and counted on average 4 infectious centers in the negative control siRNA-treated cells while no infectious center, or infected cell, was detected in nectin-4 siRNA treated cells (**Figure 3c**). Thus MV infection depends on the presence of nectin-4.

A second assay of nectin-4 function in well-differentiated human airway epithelia relied on MV-nectin4<sup>blind</sup> (originally named MV-EpR<sup>blind</sup>), a virus with two amino acid mutations in its H protein disallowing cell entry through the epithelial receptor<sup>13</sup>. **Supplementary Fig. 4** documents that while MV infectious centers included more than 100 cells, the rare MV-nectin4<sup>blind</sup> infections were limited to 1-2 cells. Thus MV must recognize nectin-4 to enter human airway epithelial sheets, and to efficiently spread laterally.

The fact that nectin-4 is transcribed at the highest level in the trachea<sup>8</sup> prompted us to consider a mechanism targeting virus emergence to the tracheobronchial airways. To analyze whether MV replicates in nectin-4 expressing cells in an infected host, we inoculated cynomolgus monkeys (*Macaca fascicularis*) that can develop the clinical signs of measles<sup>23</sup>. To facilitate detection of infectious centers, a GFP-expressing virus was used. Tissues were collected near the peak of acute disease 12 days post-inoculation, and analyses of tracheal sections revealed the expected pathological pattern (**Supplementary Fig. 5**, panels a-d).

**Figure 4** is a correlative analysis of nectin-4 expression and MV replication in epithelia: strongly nectin-4 positive cells were located directly adjacent to infectious centers. These centers consistently included many DAPI (blue) counterstained nuclei, and always lined the tracheal lumen (**Figure 4**, two overlay panels at right; see also paraffin sections in **Supplementary Fig. 5**, panels e-g). Remarkably, within infected cells nectin-4 was sometimes expressed at low levels, suggesting virus-induced downregulation. Indeed **Supplementary Fig. 6** documented that median nectin-4 cell surface expression in infected lung and bladder epithelial cell lines is about 5 times lower than in uninfected cells.

Having considered that in cells where nectin-4 is not expressed MV replication cannot occur, we assessed the levels of viral nucleocapsid and nectin-4 mRNA in the trachea and lung tissues of the five infected animals by real-time PCR. **Supplementary Fig. 7** documents a high correlation coefficient ( $r=0.77$ ) between viral and nectin-4 mRNA levels. Moreover, it indicates high nectin-4 expression levels in the trachea and lungs, suggesting that nectin-4 distribution in the airways of cynomolgus macaques is similar to humans.

MV begins its circuit through selected organs of the human body within SLAM-expressing alveolar macrophages and dendritic cells, which ferry it through the epithelial barrier<sup>3,4</sup> (**Supplementary Fig. 8**). Analyses in primate models indicate that vigorous MV replication occur in primary and secondary lymphatic organs, including tracheobronchial lymph nodes, already 3-5 days after infection<sup>4</sup>. A few days' later, most infected cells in the trachea are of lymphoid or myeloid origin, and located in the sub-epithelial cell layer<sup>24</sup>. We collected here tissues at the peak of acute disease, and documented large infectious centers in nectin-4 expressing epithelial cells adjacent to the tracheal lumen. We also observed good correlation between MV and nectin-4 mRNA levels in different parts of the lungs. These data and the experimental demonstration that a virus unable to recognize nectin-4 cannot cross the airway epithelium and is not shed<sup>13</sup>, are consistent with targeting of a protein expressed in the trachea for site-directed host exit. Emergence into the tracheobronchial airways appears ideal for aerosol droplet release through coughing and sneezing, filling the air with virus

particles ready to infect the next host, and accounting for the extraordinary high reproductive rate of MV in naïve populations<sup>25</sup>.

Nectin-4 is highly expressed in lung, breast and ovarian cancer, for which it is used as a marker<sup>9-11</sup>. MV replicates preferentially in cancer cells<sup>26</sup>, and spontaneous regressions of different forms of lymphoma were repeatedly observed after natural MV infections. These oncolytic effects are attributed to SLAM-overexpression in transformed lymphocytes<sup>6</sup>. On the other hand, a vaccine-lineage MV, which recognizes ubiquitous CD46 in addition to SLAM as receptor, is currently used in ovarian cancer clinical trials<sup>12</sup>. Since most ovarian cancers are of epithelial origin, nectin-4 expression is worth testing as a retrospective correlate of MV oncolytic activity. In addition, MV-based clinical trials of lung and breast cancer should be considered. Interestingly, most viruses in oncolysis clinical trials<sup>26</sup> exploit junction proteins as receptors<sup>27</sup>. It is conceivable that general accessibility of junction proteins in disordered cancer tissue facilitates viral entry, contributing to efficient oncolysis.

## Methods Summary

### Viruses

All three GFP-expressing recombinant viruses used here were derived from the wild-type IC-B strain infectious cDNA<sup>28</sup>. They were rescued<sup>29</sup>, amplified and titered as described previously<sup>13</sup>.

### Cells

The human lung cell lines H358 (catalog no. CRL-5807; ATCC), H441 (HTB-174), H23 (CRL-5800), H522 (CRL-5810), and Calu-3 (HTB-55), and the human bladder cell lines SCaBER (HTB-3), T24 (HTB-4), and HT-1376 (CRL-1472) were maintained as instructed by ATCC. The rescue helper cell line 293-3-46<sup>29</sup> was grown in DMEM with 10% FCS and 1.2 mg/ml of G418. Vero/hSLAM cells were kindly provided by Y. Yanagi (Kyushu University, Fukuoka, Japan). Transgenic CHO-nectin1, CHO-nectin2, CHO-nectin4, and CHO-PVR cells were maintained as instructed<sup>10,30</sup>. Expression of the nectin family proteins on these cells was confirmed with specific antibodies.

Online methods include RNA profiling; gene expression knock-down; FACS analysis; fusion assays; inhibition of syncytia formation; overlay binding assays; BIAcore; establishment and infection of airway epithelial sheets; primate infection and histology.

## Supplementary Material

Refer to Web version on PubMed Central for supplementary material.

## Acknowledgements

We thank Janina Brüning, Arthur Schnoor Cancio, Ashley Peterson, Isabelle Meunier and Chantal Thibault for technical assistance; Yusuke Yanagi for Vero-hSLAM cells and p(+)MV323-EGFP; Thilo Stehle for soluble SLAM; Jocelyn Fournier and Gary Kobinger for facilitating the macaque studies; Renate König, Dagmar Schilling-Leiß, and Tanner Miest for helpful discussions. Dedicated to Heinz Schaller (1932-2010) from one of his students. This work was supported by grants BMG 2510-FSB-705 to MDM; NIH R01 AI063476 and NIH R01 CA090636 to RC; the Roy J. Carver Charitable Trust, Cell Culture Core and Cell Morphology Cores, partially supported by the Center for Gene Therapy for Cystic Fibrosis (NIH P30 DK-54759), and the Cystic Fibrosis Foundation to PBM;

CIHR MOP-66989 and CFI 9488 to VvM; INSERM, Institut Paoli-Calmettes, and LNCC (label 2009-2011) to ML. XXW was supported by a CIHR Master's Award.

## Online Methods

### RNA profiling

Data from the first round of profiling were analyzed by the Department of Biomedical Informatics at Mayo Clinic. After data normalization and determination of the sensitivity of the array, 21,163 probe sets were compared for transcript expression (average permissive/average non permissive). The data were further filtered for membrane-associated proteins, resulting in a list of 1,531 probe sets. A total of 254 probe sets, representing 175 proteins, were overexpressed at least 5 times in the cells permissive to wild type MV compared to non-permissive cells. Of these 22 were expressed; the complete list of these proteins is presented in a footnote of **Supplementary Table 1**. This Table also presents the data from the second round of profiling. Here, quality-verified RNA of all previously characterized 7 epithelial cell lines<sup>13</sup> were prepared in triplicates and analyzed with Agilent's Microarray Scanner System based on the one-color Agilent 60-mer oligo microarray processing protocol (Agilent Technologies, Miltenyi Biotech, Bergisch Gladbach, Germany). Detected signals of probe sets (41,000) were normalized and signal intensities were compared for transcript expression (median permissive versus median non-permissive) resulting in 2,952 up-regulated probe sets in permissive cells. These were further filtered for membrane-associated proteins (259 probe sets), representing 222 up-regulated proteins. The table presents a selection of these 222 proteins sorted for the median distance (last row) of permissive versus non-permissive cells' signal intensities, expressed as log<sub>2</sub> values. The respective factor of mRNA overexpression in permissive cells, i.e. the total signal intensity differences, can be deduced by calculating factor 2 to the power of the median distance. Microarray data are available in the GEO database with the accession number GSE32155.

### Gene expression knock-down

The most effective siRNAs directed against nectin-4 mRNA was Hs\_PVRL4\_1 (target sequence CAGAGCAGTATTAATGATGCA; FlexiTube GeneSolution for PVRL4). This siRNA as well as negative (AllStars Negative Control siRNA) and positive control (AllStars Hs Cell Death siRNA) siRNA duplexes were purchased from QIAGEN (Hilden, Germany). siRNA was transfected into H358 cells using Lipofectamine RNAiMAX reagent (Invitrogen, Darmstadt, Germany) according to manufacturer's instructions. Briefly,  $4.5 \times 10^3$  cells were reversely transfected in 96-well plates using 3 pmol of the respective siRNA with 0.15  $\mu$ l transfection reagent in a total volume of 90  $\mu$ l. Transfected cells were cultured for 48 hrs before infection or analysis. Unspecific side effects of the siRNAs were assessed in the CD46-expressing H358 cells with a CD46-recognizing MV, which entry was not affected.

### FACS analysis

Cells ( $5 \times 10^5$ ) were detached with PBS-EDTA (2 mM) and washed three times with cold phosphate buffered saline, incubated (1 hour) with 1  $\mu$ g/ml PVRL4 mouse anti-human monoclonal (amino acid 27-351) antibody (LS-C37483; Lifespan Biosciences, Seattle, WA,

USA), or MST1R antibody ab52927 (Abcam, Cambridge, UK) or mouse IgG1 isotype control antibody (BD Bioscience, Heidelberg, Germany) in FACS-wash buffer (PBS + 2% FCS + 0.1% NaN<sub>3</sub>). Cells were washed three times with FACS-wash buffer and incubated for one hour with PE-labeled goat anti-mouse IgG secondary antibody (BD Bioscience) diluted 1:50 in FACS-wash buffer. After washing cells three times with FACS-wash buffer, cells were fixed with PBS + 2% PFA and subsequently analyzed on a LSRII-SORP FACS analyzer and Diva software (BD Bioscience).

## Fusion assays

Cells seeded in 6-well tissue culture plates were allowed to reach 80% confluence prior to transfection. Equal amounts (1 µg) of pCG-IC323-F, the mutated pCGIC323-H, and EGFP-expressing pEGFP-N1 (BD Biosciences) were transfected in presence or absence of 1 µg pcDNA3.1-PVRL4 using FuGENE HD (Roche) according to the manufacturer's protocol. Twenty-four to 48 hours post transfection, the formation of syncytia was observed under a fluorescence microscope.

## Inhibition of syncytia formation

MV-induced syncytia were counted on  $2 \times 10^4$  H358 cells/well in a 96-well dish. The day after seeding, cells were washed and medium added with different concentrations of the N4.40 or N4.61 antibodies, or different concentrations of the soluble N4VCC or N4V; 100 TCID<sub>50</sub>/ml per well of a recombinant MVwt323-GFP(N) were added simultaneously. Two days after infection, syncytia formation was observed under a fluorescence microscope and the number of syncytia per well was counted.

## Overlay binding assays

In the glycoprotein overlay binding assay, 0.1 µg of recombinant SLAM, N4VCC or N4V were separated on 8% non-reducing SDS-PAGE. After transfer to a PVDF membrane and blocking overnight, membranes were incubated for 45 min with a soluble H ectodomain (sH, amino acids 60-617)<sup>20</sup>. In the virus overlay protein binding assay, 0.1 µg of recombinant SLAM, N4VCC or N4V were separated on 8% SDS-PAGE. After transfer to a PVDF membrane and blocking overnight, membranes were incubated for 45 min with  $5 \times 10^4$  TCID<sub>50</sub> of a recombinant MVwt323-GFP(N). After washing, the membranes were revealed using primary antibodies against H and corresponding secondary antibodies.

## BIAcore

Soluble H ectodomain (amino acids 60-617) and soluble SLAM (amino acids 21–230, the complete ectodomain) were expressed and purified as described<sup>20</sup>. Soluble nectin-4 ectodomain fused to human IgG1 Fc domain was expressed and purified as described<sup>8</sup>. The interaction of the sH-protein with sSLAM and nectin-4-Fc was monitored by surface plasmon resonance using a BIAcore 3000 instrument and CM5 sensor chips (GE Healthcare) and the data analyzed using the BIAevaluation 4.1 software as described<sup>20</sup>.

## Establishment, transfection and infection, of polarized human airway epithelial cells

Primary cultures of human airway epithelia were prepared from trachea and bronchi by enzymatic dispersion and seeded onto collagen-coated, semipermeable membranes with an 0.4- $\mu\text{m}$  pore size (Millicell-HA; surface area, 0.6  $\text{cm}^2$ ; Millipore Corporation) as previously described<sup>21</sup>. Only well-differentiated cultures (>2 weeks old; resistance, >500 Ohms/ $\text{cm}^2$ ) were used. Transepithelial resistance was measured with a volt-ohm meter (World Precision Instruments). Values were corrected for the blank filter resistance and further standardized against baseline readings and uninfected cultures. Neither corrected nor raw numbers resulted in a statistically significant variation from measurements in uninfected epithelia as determined by ANOVA. For transfections, Costar transwell permeable supports (3470 clear) were coated overnight with collagen and washed the following day with PBS (1% Penicillin-Streptomycin). 200,000 freshly dissociated human tracheal epithelial cells were transfected in each transwell using Lipofectamine RNAiMAX with 100 nM dsRNA oligonucleotides: 5'-GCAGUAUUAUGAUGCAGAGGUUGG-3' and 5'-CCAACCUCUGCAUCAUUAUACUGCUC-3'. Apical media was aspirated 6 hrs post-transfection and Ultrosor G (Pall corporation) media was added to the basolateral surface. For infections, MV preparations were diluted in sterile PBS to a multiplicity of infection (MOI) of 0.1 (as determined on Vero-SLAM cells), and 100  $\mu\text{l}$  of the solution was applied to the basolateral surface. We did note that human airways polarized, well-differentiated cells have a much lower susceptibility to MV infection than Vero-SLAM cells. This was expected since these transformed cells have reduced innate immunity, including the absence of interferon responses, and their barriers to infection are reduced compared to a differentiated epithelium.

## Primate infection and histology

Five adult female cynomolgus macaques (*M. fascicularis*) were infected intranasally with  $10^5$  tissue culture infectious doses (TCID<sub>50</sub>) of wild type MV expressing GFP and euthanized after 12 days. The institutional animal care and use committee of the INRS-Institut Armand-Frappier (#1007-07) approved all experiments. Tissue samples were harvested and either immediately frozen at -80°C or fixed in 4% paraformaldehyde (Sigma) for at least 48 hrs. Fixed trachea samples were either paraffin-embedded cut in 5  $\mu\text{m}$  sections and used for hematoxylin and eosin staining or immunostained using a monoclonal antibody against MV nucleoprotein (MAB8906, Millipore), a monoclonal antibody against nectin-4 (MAB2659, R&D) or a universal negative control for mouse IgG (N1698, Dako) and counterstained with hematoxylin, or OCT-embedded, cut in 8  $\mu\text{m}$  sections using a cryostat, and counterstained with 4',6-diamidino-2-phenylindole (DAPI).

## REFERENCES

1. Vaccines: the case of measles. *Nature*. 2011; 473:434–435. doi:10.1038/473434a. [PubMed: 21614052]
2. Chen SY, et al. Health care-associated measles outbreak in the united states after an importation: challenges and economic impact. *J Infect Dis*. 2011 doi:10.1093/infdis/jir115.

3. Ferreira CS, et al. Measles virus infection of alveolar macrophages and dendritic cells precedes spread to lymphatic organs in transgenic mice expressing human signaling lymphocytic activation molecule (SLAM, CD150). *J Virol.* 2010; 84:3033–3042. doi:10.1128/JVI.01559-09. [PubMed: 20042501]
4. Lemon K, et al. Early target cells of measles virus after aerosol infection of non-human primates. *PLoS Pathog.* 2011; 7:e1001263. doi:10.1371/journal.ppat.1001263. [PubMed: 21304593]
5. Leonard VH, Hodge G, Reyes-Del Valle J, McChesney MB, Cattaneo R. Measles virus selectively blind to signaling lymphocytic activation molecule (SLAM; CD150) is attenuated and induces strong adaptive immune responses in rhesus monkeys. *J Virol.* 2010; 84:3413–3420. doi:10.1128/JVI.02304-09. [PubMed: 20071568]
6. Tatsuo H, Ono N, Tanaka K, Yanagi Y. SLAM (CDw150) is a cellular receptor for measles virus. *Nature.* 2000; 406:893–897. doi:10.1038/35022579. [PubMed: 10972291]
7. de Swart RL, et al. Predominant infection of CD150+ lymphocytes and dendritic cells during measles virus infection of macaques. *PLoS Pathog.* 2007; 3:e178. doi:10.1371/journal.ppat.0030178. [PubMed: 18020706]
8. Reymond N, et al. Nectin4/PRR4, a new afadin-associated member of the nectin family that trans-interacts with nectin1/PRR1 through V domain interaction. *J Biol Chem.* 2001; 276:43205–43215. doi:10.1074/jbc.M103810200. [PubMed: 11544254]
9. Derycke MS, et al. Nectin 4 overexpression in ovarian cancer tissues and serum: potential role as a serum biomarker. *Am J Clin Pathol.* 2010; 134:835–845. doi:10.1309/AJCPGXK0FR4MHIHB. [PubMed: 20959669]
10. Fabre-Lafay S, et al. Nectin-4, a new serological breast cancer marker, is a substrate for tumor necrosis factor-alpha-converting enzyme (TACE)/ADAM-17. *J Biol Chem.* 2005; 280:19543–19550. doi:10.1074/jbc.M410943200. [PubMed: 15784625]
11. Takano A, et al. Identification of nectin-4 oncoprotein as a diagnostic and therapeutic target for lung cancer. *Cancer Res.* 2009; 69:6694–6703. doi:10.1158/0008-5472.CAN-09-0016. [PubMed: 19679554]
12. Galanis E, et al. Phase I trial of intraperitoneal administration of an oncolytic measles virus strain engineered to express carcinoembryonic antigen for recurrent ovarian cancer. *Cancer Res.* 2010; 70:875–882. doi:10.1158/0008-5472.CAN-09-2762. [PubMed: 20103634]
13. Leonard VH, et al. Measles virus blind to its epithelial cell receptor remains virulent in rhesus monkeys but cannot cross the airway epithelium and is not shed. *J Clin Invest.* 2008; 118:2448–2458. doi:10.1172/JCI35454. [PubMed: 18568079]
14. Wagner KW, et al. Death-receptor O-glycosylation controls tumor-cell sensitivity to the proapoptotic ligand Apo2L/TRAIL. *Nat Med.* 2007; 13:1070–1077. doi:10.1038/nm1627. [PubMed: 17767167]
15. Fabre S, et al. Prominent role of the Ig-like V domain in trans-interactions of nectins. Nectin3 and nectin 4 bind to the predicted C-C'-C''-D beta-strands of the nectin1 V domain. *J Biol Chem.* 2002; 277:27006–27013. doi:10.1074/jbc.M203228200. [PubMed: 12011057]
16. Brancati F, et al. Mutations in PVRL4, encoding cell adhesion molecule nectin-4, cause ectodermal dysplasia-syndactyly syndrome. *Am J Hum Genet.* 2010; 87:265–273. doi:10.1016/j.ajhg.2010.07.003. [PubMed: 20691405]
17. Mendelsohn CL, Wimmer E, Racaniello VR. Cellular receptor for poliovirus: molecular cloning, nucleotide sequence, and expression of a new member of the immunoglobulin superfamily. *Cell.* 1989; 56:855–865. [PubMed: 2538245]
18. Campadelli-Fiume G, Cocchi F, Menotti L, Lopez M. The novel receptors that mediate the entry of herpes simplex viruses and animal alphaherpesviruses into cells. *Rev Med Virol.* 2000; 10:305–319. [PubMed: 11015742]
19. Noyce RS, et al. Tumor cell marker PVRL4 (Nectin 4) is an epithelial cell receptor for measles virus. *PLoS Pathog.* 2011; 7:e1002240. doi:10.1371/journal.ppat.1002240. [PubMed: 21901103]
20. Navaratnarajah CK, et al. Dynamic interaction of the measles virus hemagglutinin with its receptor signaling lymphocytic activation molecule (SLAM, CD150). *J Biol Chem.* 2008; 283:11763–11771. doi:10.1074/jbc.M800896200. [PubMed: 18292085]

21. Karp PH, et al. An in vitro model of differentiated human airway epithelia. Methods for establishing primary cultures. *Methods Mol Biol.* 2002; 188:115–137. doi:10.1385/1-59259-185-X:115. [PubMed: 11987537]
22. Tahara M, et al. Measles virus infects both polarized epithelial and immune cells by using distinctive receptor-binding sites on its hemagglutinin. *J Virol.* 2008; 82:4630–4637. doi:10.1128/JVI.02691-07. [PubMed: 18287234]
23. Welshman MD. Measles in the cynomolgus monkey (*Macaca fascicularis*). *Vet Rec.* 1989; 124:184–186. [PubMed: 2929098]
24. Ludlow M, et al. Wild-type measles virus infection of primary epithelial cells occurs via the basolateral surface without syncytium formation or release of infectious virus. *J Gen Virol.* 2010; 91:971–979. doi:10.1099/vir.0.016428-0. [PubMed: 19923259]
25. Monto AS. Interrupting the transmission of respiratory tract infections: theory and practice. *Clin Infect Dis.* 1999; 28:200–204. doi:10.1086/515113. [PubMed: 10064226]
26. Cattaneo R, Miest T, Shashkova EV, Barry MA. Reprogrammed viruses as cancer therapeutics: targeted, armed and shielded. *Nat Rev Microbiol.* 2008; 6:529–540. doi:10.1038/nrmicro1927. [PubMed: 18552863]
27. Bergelson JM. Intercellular junctional proteins as receptors and barriers to virus infection and spread. *Cell Host Microbe.* 2009; 5:517–521. doi:10.1016/j.chom.2009.05.009. [PubMed: 19527879]
28. Takeda M, et al. Recovery of pathogenic measles virus from cloned cDNA. *J Virol.* 2000; 74:6643–6647. [PubMed: 10864679]
29. Radecke F, et al. Rescue of measles viruses from cloned DNA. *Embo J.* 1995; 14:5773–5784. [PubMed: 8846771]
30. Reymond N, et al. DNAM-1 and PVR regulate monocyte migration through endothelial junctions. *J Exp Med.* 2004; 199:1331–1341. doi:10.1084/jem.20032206. [PubMed: 15136589]

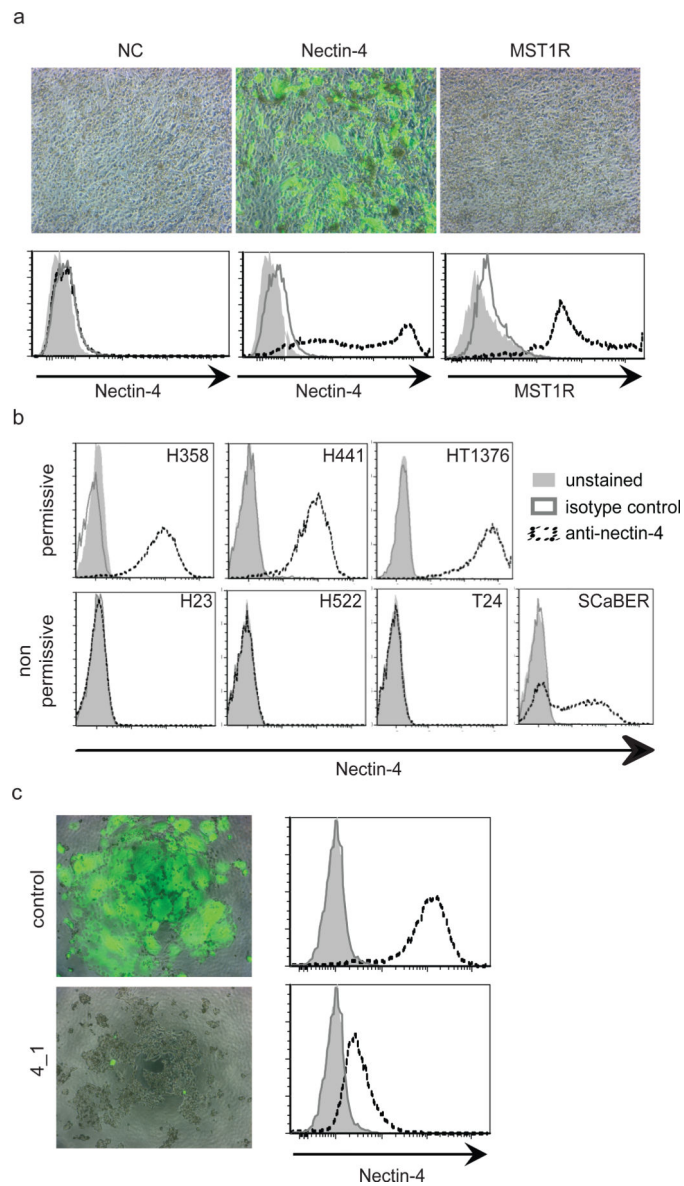


**Figure 1. Identification of nectin-4 as candidate MV receptor**

**a**, Nectin-4 mediates MV entry. CHO-K1 cells were not transfected (mock), or transfected with the expression plasmids nectin-4 or MST1R. Top row: after transfection cells were infected with a MV expressing GFP. Bottom row: expression of nectin-4 and MST1R (interrupted black lines), as documented by FACS analysis. Dark grey lines: isotype controls; light grey shadings: unstained controls. **b**, FACS analysis of nectin-4 expression levels in different cells. Cell lines H358, H441 and HT1376, top row, are permissive for MV infection. Cell lines H23, H522, T24, and SCaBER are non-permissive. Antibody LS-C37483 was used. **c**, siRNA-mediated knock-down of nectin-4 expression in H358 cells (left panels). Control (top row) or nectin-4 specific 4\_1 siRNA (bottom row) were transfected. After transfections cells were infected with a MV expressing GFP. FACS analysis (right panels) indicated more than 90% reduction of nectin-4 expression on the cell surface.

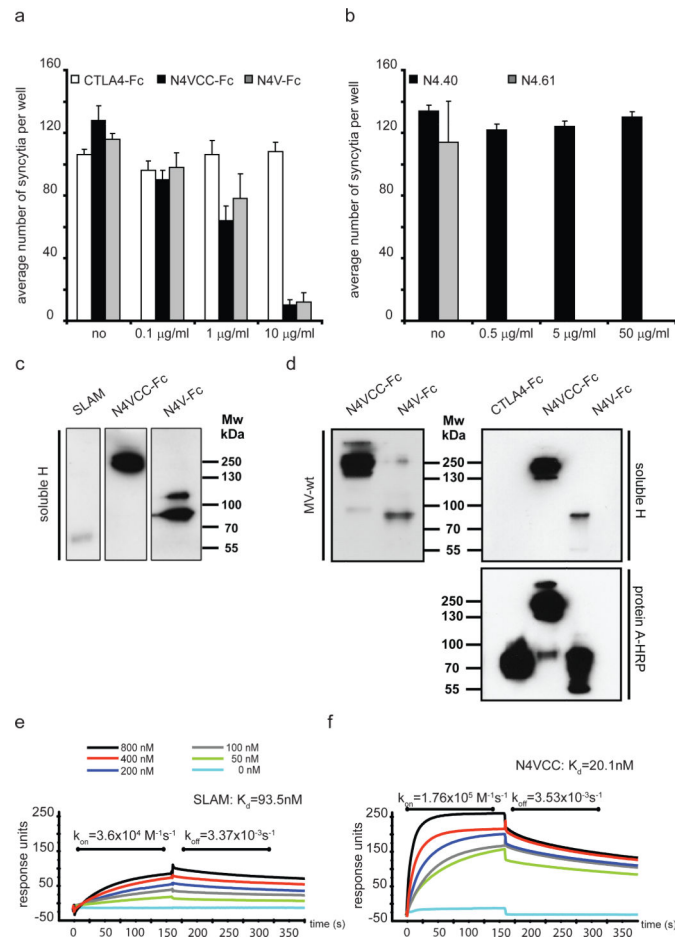


### Figure 2. V domain of nectin-4 supports strong binding to MV H

**a** and **b**, MV infection competition assays in H358 cells. For (**a**), N4VCC-Fc (grey bars) with all three immunoglobulin domains, and N4V-Fc (black bars) with only the V domain were used. As control soluble immunoglobulin superfamily protein CTLA4-Fc (cytotoxic T lymphocyte antigen 4, also named CD152) was used (white bars). For (**b**), antibodies N4.40, recognizing one of the C domains, or N4.61 recognizing the V domain, were used. All assays were done in triplicate ( $n=3$ ); mean and standard deviation of the number of observed syncytia per well are indicated on the vertical axis. Concentration of the undiluted protein solution is indicated on the horizontal axis. For dimeric N4VCC-Fc 10  $\mu\text{g/ml}$  are 71 nM; no, no protein added. **c** and **d**, non-reducing gel electrophoresis analysis of binding of soluble H and purified virus particles to different soluble receptors. Molecular weight markers are indicated. N4VCC-Fc and N4V-Fc are dimeric proteins of 140 kDa and 90 kDa respectively<sup>8</sup>. The 260 kDa observed for N4VCC-Fc probably corresponds to association of two dimers through C domain dependent homophilic interactions. For (**d**), CTLA4-Fc loaded at the same concentration did not cross-react with soluble H (right top panel), but was detected by protein A-HRP with the same efficiency (right bottom panel). **e**, surface plasmon resonance analyses of H binding to SLAM. Multiple cycles of association and dissociation were performed using receptor concentrations ranging from 50 to 800 nM

(color coding on top). Horizontal axis: time in seconds; vertical axis, absorbance units. **f**, surface plasmon resonance analyses of H binding to nectin-4.

Author Manuscript

Author Manuscript

Author Manuscript

Author Manuscript



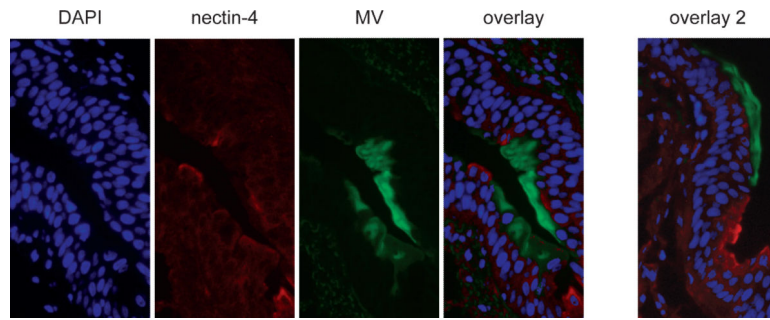


**Figure 4. Nectin-4 expression and infection of monkey tracheal epithelium**

Microscopic analyses of tracheal tissue obtained from cynomolgus macaques 12 days after inoculation with MV. From left to right: nuclear staining by DAPI (blue); nectin-4 staining with a mixture of two antibodies (red); MV infection revealed through GFP expression (green); overlay of the three panels; overlay of three panels of another section (overlay 2). Frozen sections were photographed at 4000-fold magnification with oil immersion.